Inelastic electron scattering from^{64}Ni

Blok, H.P.; Braunstein, M.R.; de Vries, H.; Kraushaar, J.J.; Michel, R.P.; Mitchell, J.H.; Peterson, R.J.

published in
Physical Review C
1988

PHYSICAL REVIEW C VOLUME 37, NUMBER 5 MAY 1988

Inelastic electron scattering from ^{64}Ni

M. R. Braunstein, J. J. Kraushaar, R. P. Michel, J. H. Mitchell,* and R. J. Peterson
Nuclear Physics Laboratory, Department of Physics, University of Colorado, Boulder, Colorado 80309

H. P. Blok
Natuurkundig Laboratorium, Vrije Universiteit, 1009 MC Amsterdam, The Netherlands
and Sektie Kernfysica, Nationaal Instituut voor Kernfysica en Hoge-Energiefysica, 1009 AJ Amsterdam, The Netherlands

H. de Vries
Sektie Kernfysica, Nationaal Instituut voor Kernfysica en Hoge-Energiefysica, 1009 AJ Amsterdam, The Netherlands
(Received 21 December 1987)

Elastic and inelastic electron scattering has been carried out on ^{64}Ni with $q_{\rm eff}$ ranging from 0.40 to 1.15 fm^{-1}. Twenty-seven states up to an excitation energy of 6.2 MeV have been identified and spin assignments and electromagnetic transition rates established for 22 states. The comparison of the excitation strengths from electron and alpha particle scattering is not in agreement with the hydrodynamic model for the first 3^- transition, but is nearly as expected for the first 2^+ transition.

I. INTRODUCTION

The level structure of ^{64}Ni has been studied little, which is a serious lack for a nucleus where the protons have just filled the major shell of $Z=28$. This fact is no doubt related to the low abundance of ^{64}Ni (1.08%) among the nickel isotopes. In our study of the giant quadrupole resonances by inelastic electron scattering on a series of nuclei, information was acquired on the form factors for a number of low-lying states in ^{64}Ni that had not previously been studied. Twenty-seven states could be identified, and spin and electromagnetic transition rates established for 22 states in the electron scattering data. The momentum transfer ranged from 0.40 to 1.15 fm^{-1}.

Existing information on the levels of ^{64}Ni had been summarized by Halbert[1] in 1979. Table I lists the adopted energies, spins, and parities of the levels that are relevant to this study. The energies of the levels are based mainly on detailed (p,p′) and (p,p′γ) studies[2,3] using low energy protons. Since 1979 there have been two studies that have provided some additional information about the low-lying levels of ^{64}Ni. Albinski *et al.*[4] determined, using inelastic alpha particles scattering at 172.5 MeV, the isoscalar transition rates for the prominent collective states at 1.35(2^+), 2.60(4^+), and 3.58(3^-) MeV. These results will be compared later to those from the present inelastic electron scattering experiment. Jahn *et al.*,[5] using the (α,^{2}He) reaction, identified several high-spin, two-neutron states at 4.60(7^+), 5.81(8^+), and 6.03(6^+) MeV. These states were not observed in this paper.

II. EXPERIMENTAL PROCEDURE

The experiment was performed with the electron-scattering facility at Sektie Kernfysica, Nationaal Instituut voor Kernfysica en Hoge-Energiefysica (NIKHEF-K) using the high-resolution quadrupole-dipole-dipole spectrometer.[6] Incident energies of 147.4, 200.0, 225.0, and 356.0 MeV were used at scattering angles ranging from 29° to 56° to provide values of the effective momentum transfer of 0.40, 0.52, 0.64, 0.73, 0.87, 1.00, and 1.15 fm^{-1} for elastic scattering from ^{64}Ni. The ^{64}Ni target was in the form of a metallic foil with an areal density of 100.3 mg/cm^2 and an enrichment of 97.9%. The energy resolution obtained with the ^{64}Ni target was about 33 keV full width at half maximum (FWHM) which was almost completely due to the target thickness. Targets of ^{118}Sn, ^{90}Zr, ^{12}C, and BeO were used for calibration purposes. The beam currents ranged up to 35 μA. The collected charge was obtained by integrating signals from a toroid monitor around the electron beam.

Analysis of the data began by fitting the peaks in the spectra from both the ^{64}Ni and the four targets used for calibration. Only peaks that were well defined and that corresponded to states with well-established energies were included. For each momentum transfer the centroids and known energies were then used to obtain the focal plane calibration. This was then utilized in the program BINSOR (Ref. 7) to transform the on-line data into physical spectra based directly on excitation energy. The resulting spectra were then analyzed using the program ALLFIT,[8] with which a detailed fit of all of the peaks in the spectra could be obtained including contributions from the radiative tails. The elastic peak was fit first.

The shape of the elastic peak was then fixed and used for all of the other sharp peaks in the spectrum for which the area and excitation energy were determined. Aside from the strong 1.345 MeV 2^+ and 3.560 MeV 3^- states, most of the states could only be seen clearly in the four or five spectra taken at the larger momentum transfers. The excitation energies quoted in Table I are the average values for the several determinations. The uncertainties in the quoted values are about 3 keV for the stronger states and about 6 keV for the weaker states.

A spectrum taken at $q_{eff}=1.15$ fm^{-1} is shown in Fig. 1. The continuous line shown is the fit to the data generated using ALLFIT and the energies of the states are shown in keV above the corresponding peaks. Most of the states that were seen in the present experiment correspond very well to states seen previously.[1] In Table I only the states from the earlier (p,p′) and (p,p′γ) studies[2,3] that were close in energy to states seen in the present work are listed. Typical uncertainties in excitation energy from these earlier results are ±7 keV.

III. RESULTS

The results for the elastic scattering on ^{64}Ni are shown in Fig. 2. The statistical uncertainty in the data is less than the size of the data points. The solid line is the calculated form factor using a Gaussian model charge distribution[9] with parameters $c=3.842$ fm, $z=2.346$ fm, and $w=0.333$. The effects of target thickness and the finite solid angle of the spectrometer have been taken into account in these calculations. It can be seen that the overall agreement between the measured and calculated form factors is acceptable and that no renormalization of the data is required. Since the goal of this paper is to examine inelastic transitions, and the range of momentum transfers was small, no attempt was made to reanalyze the ground state charge distribution.

The form factors for the states that are thought to have a spin and parity of 2^+ are shown in Figs. 3 and 4. The states at 1346 and 3276 keV have previously been assigned[1] as 2^+ but the other five at 4493, 4567, 4636, 4993, and 5408 keV are unassigned. Also listed in Table I are values of $B(CL)\uparrow$, the longitudinal reduced transition probabilities that have been extracted from the data by a least-squares fit to the curves as shown. No Rosenbluth decomposition of the data were performed, but at the relatively small scattering angles of this work the transverse contribution is assumed to be small. Values of $B(CL)\uparrow$ were obtained by a least squares fit of the calculated form factor to the data, with theoretical form factors calculated in the distorted-wave Born approximation (DWBA) using the program FOUBES.[10] Form factors shown by the solid curves for each multipolarity were computed using transition densities of the Tassie form, involving derivatives of the three-parameter Fermi ground states charge distribution with the same rms radius as used for elastic

TABLE I. Energy levels, spins and parities, and longitudinal reduced transition probabilities for ^{64}Ni as obtained from the present experiment and a collective analysis, using Tassie transition densities. Uncertainties in the $B(CL)$ values are only statistical. See the text for a discussion of the model dependence.

Nuclear Data Sheets[a]		Present experiment		
E_x (keV)	J^π	E_x (keV)	J^π	$B(CL)\uparrow(e^2\text{fm}^{2L})$
0.0	0^+	0.0	0^+	
1345.79	2^+	1345.5	2^+	744±20
2277.2	$(0,2)^+$		(2^+)	<2.0
2608	4^+	2610	4^+	$(224\pm6)\times10^3$
2971		2969		
3165	4^+	3163	4^+	$(72\pm6)\times10^3$
3273	2^+	3276	2^+	26±1
3393	+	3397		
3560	3^-	3561	3^-	$(31\pm1)\times10^3$
3849	5^-	3848	5^-	$(5.5\pm0.3)\times10^6$
4084	(4^+)	4076	4^+	$(37\pm3)\times10^3$
4210	+	4218	4^+	$(140\pm3)\times10^3$
4346	+	4347		
4494		4493	2^+	14±2
4567		4567	2^+	13±2
4632		4636	2^+	31±5
4720		4719	4^+	$(51\pm1)\times10^3$
4762		4760		
4894	+	4887		
4991		4993	2^+	31±2
5087	+	5095	4^+	$(164\pm6)\times10^3$
5217	+	5216	4^+	$(66\pm4)\times10^3$
5370		5369	3^-	$(2.4\pm0.2)\times10^3$
5414	−	5408	2^+	37±5
5480	+	5484	(3^-)	800±60
	−	5734	4^+	$(270\pm20)\times10^3$
		5817	3^-	870±80
		6018	3^-	$(1.40\pm0.05)\times10^3$
6121		6116	3^-	$(1.40\pm0.09)\times10^3$

[a]Reference 1. Only the states in ^{64}Ni have been listed that are related to the present study.

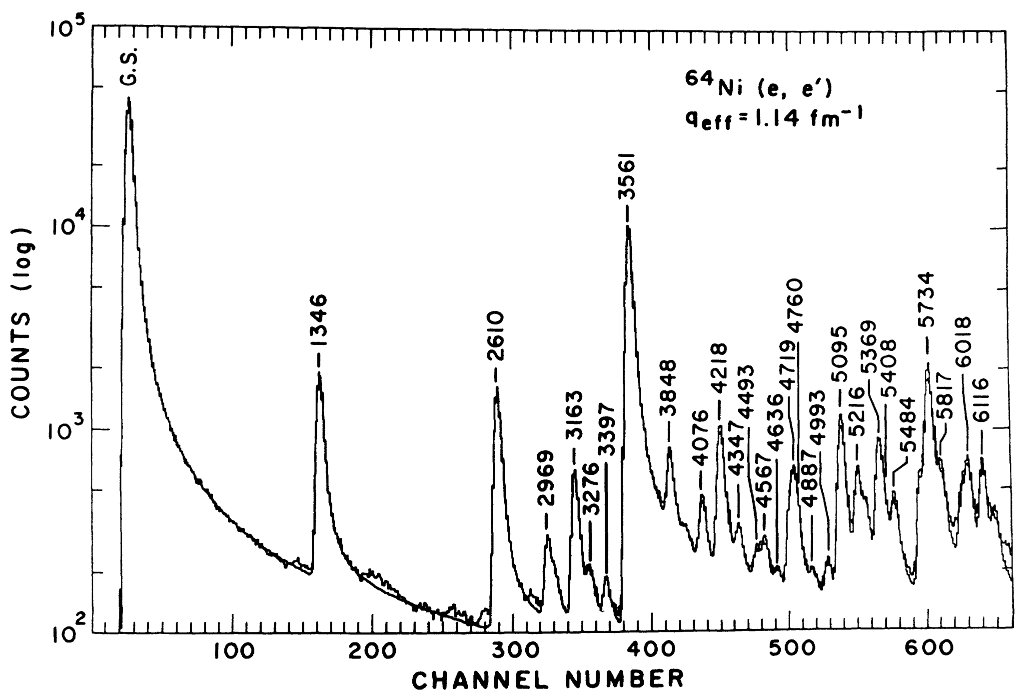

FIG. 1. Inelastic electron spectrum of ^{64}Ni. The numbers over the peaks are the excitation energies of the states in keV and the smooth line is the fit to the data.

scattering $[\rho_{tr} \propto r^{L-1}\partial\rho/\partial r]$.[9] This leaves only the normalization $B(CL)\uparrow$ to be fitted. These results are listed in Table I, and fits to the data are shown in Figs. 3–8.

The $B(CL)$ values were also determined by comparison of the data to form factors computed with a phonon transition density, proportional only to the derivative of the

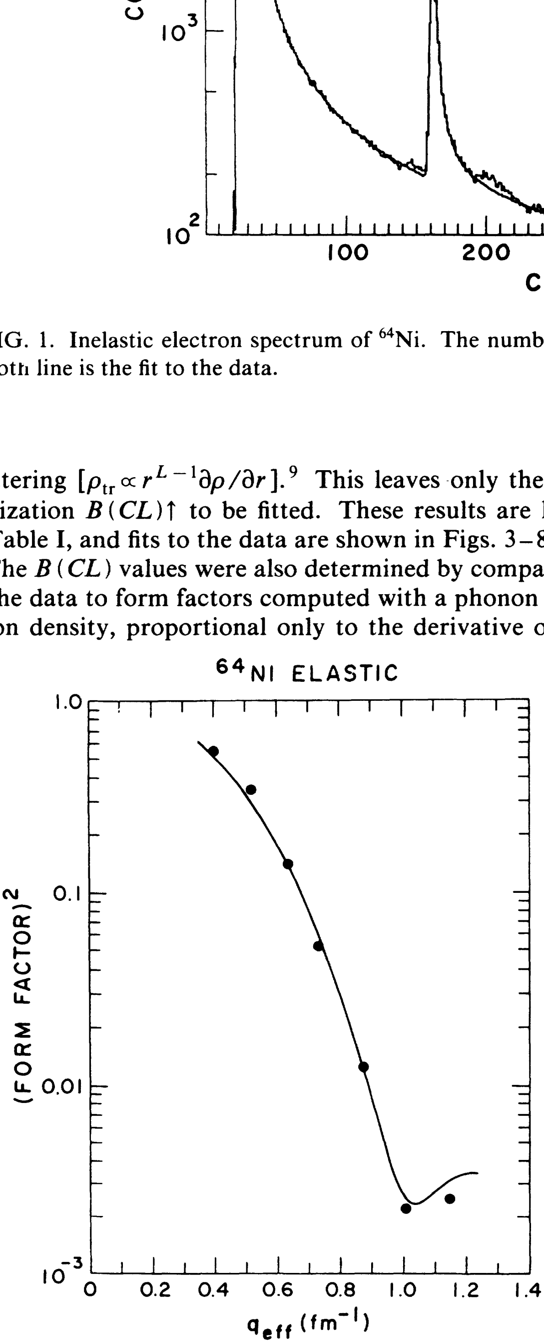

FIG. 2. Comparison of calculated and measured form factors for the elastic scattering from ^{64}Ni.

ground state charge distribution $[\rho_{tr} \propto \partial\rho/\partial r]$. This is suggested by the vibrational-like spacing of the low-lying levels of the even nickel isotopes. These fits are shown in Figs. 3, 5, 7, and 8 by the dash-dotted curves for the first 2^+, 3^-, 4^+, and 5^- states. If such derivative instead of Tassie computed form factors are used, the $B(CL)$ values in Table I should be multiplied by 0.906, 0.682, 0.594, and 0.334 for $L=2$, 3, 4, and 5, respectively, as found from the fits to the lowest states of each multipolarity. For the 5^- transition at 3.85 MeV, the solid Tassie curve yields a superior fit to the shape of the form factor, but the difference diminishes for lower multipolarities.

In order to determine the sensitivity of the extracted values of $B(CL)$ to the geometrical parameters c, z, and w used in the Tassie form factor, variations were made in each of these parameters from the values used for the elastic scattering. The parameters were each raised and lowered by 10% while holding the other two at their original value. The extreme values of $B(C2)\uparrow$ were for the first 2^+ states 737 and 749 e^2fm^4 compared to the starting value of 744 e^2fm^4. Since the variation in c were the most significant, a search was made varying that parameter while holding the other two fixed. A very broad minimum in χ^2/N was found at a value of $c=4.995$ fm yielding a value of $B(C2)\uparrow$ of 749 e^2fm^4, in excellent agreement with the simple Tassie analysis but not with the phonon analysis (674 e^2fm^4) using the ground state parameters. The Tassie mode results are reported in Table I.

Uncertainties in $B(CL)$ and matrix elements will be given from the fits shown, amounting to the statistical uncertainty of the data. An extreme model-dependent uncertainty may be estimated by the difference between Tassie and phonon models, as above.

The major octupole strength is located in the strong 3^- state at 3561 keV, with small amounts of strength for states at 5369, 5484, 5817, 6018, and 6116 keV. A number of possible 4^+ states have been located beyond the well-established 4^+ states at 2610 and 3163 keV. In Fig. 8 the form factor for the state at 3848 keV is shown. The calculated form factor for an $L=5$ transition is compared and is seen to be consistent with the few data points, which lends support to the previous[1] 5^- assignment.

There is some evidence, as can be seen in Fig. 1, for the excitation of the $(0,2)^+$ state at 2277 keV, but there were insufficient data to make a comparison to calculated form factors or to extract anything except an upper limit of 2 e^2fm^4 for $B(C2)\uparrow$.

Previous studies of transition rates in ^{64}Ni include Coulomb excitation[11] of the 1345 keV 2^+ state with a

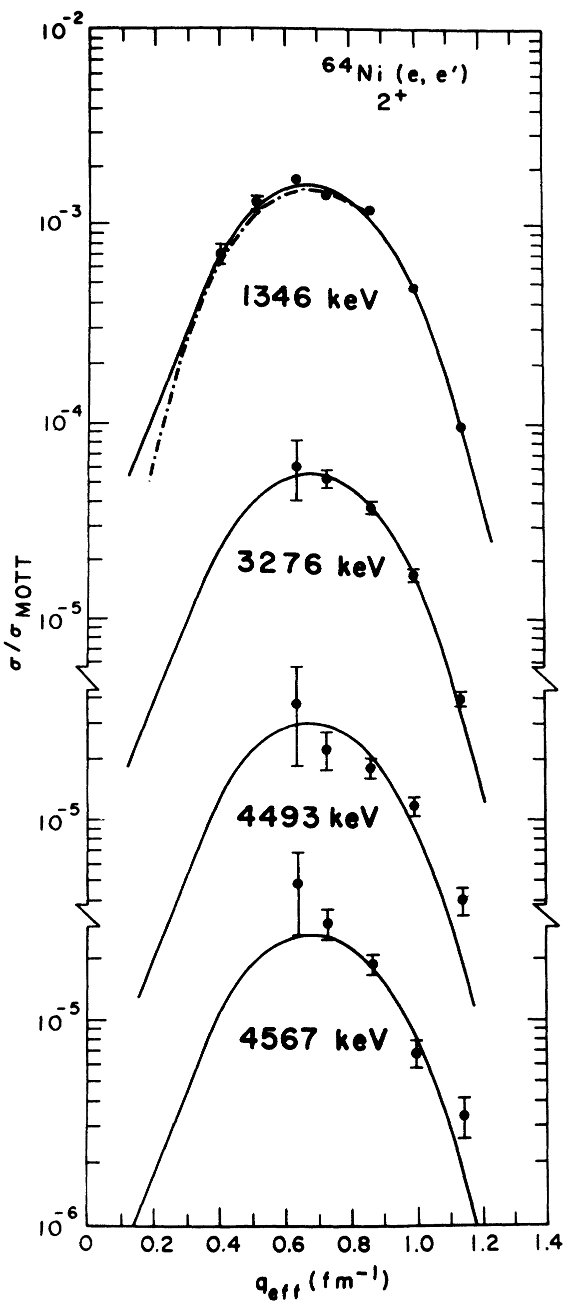

FIG. 3. Comparison of the DWBA calculated and measured form factors for the transitions to the states in ^{64}Ni that are thought to have a spin and parity of 2^+. The Tassie formulation is used for the calculations yielding the solid curves, and the phonon transition density for the dashed curves. The effective momentum transfer used for plotting purposes is given by $q_{\rm eff}=q(1+3Ze^2/2E_iR)$, with $R=6.42$ fm. The Mott cross section used is for a point charge Ze.

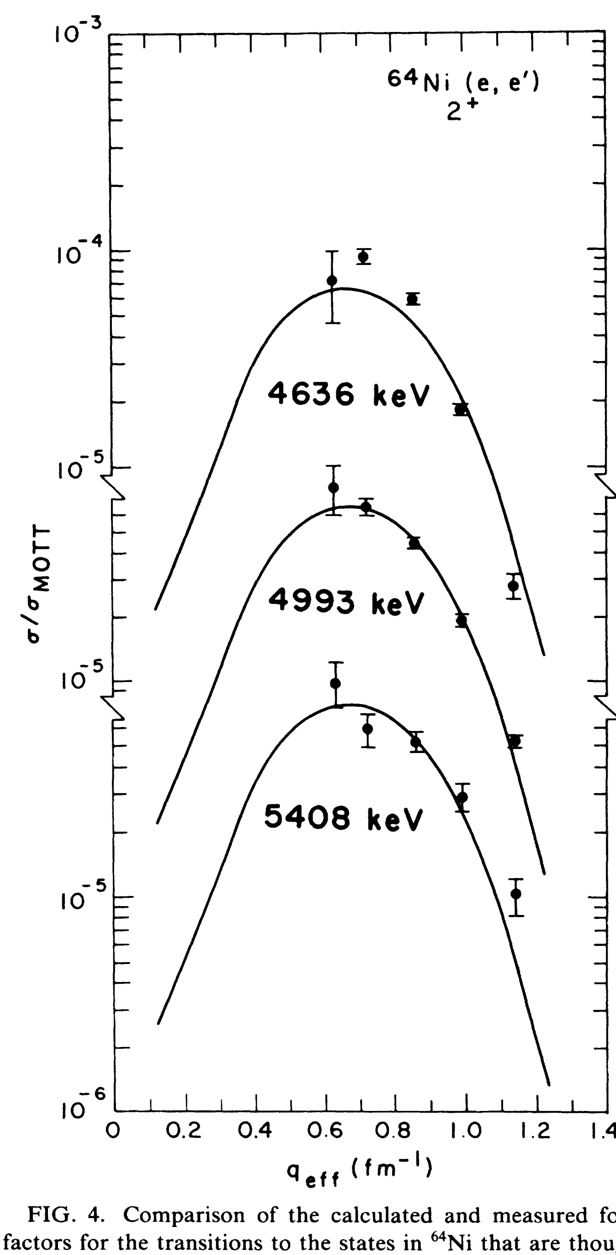

FIG. 4. Comparison of the calculated and measured form factors for the transitions to the states in ^{64}Ni that are thought to have a spin and parity of 2^+. The Tassie formulation is used for the calculations yielding the solid curves.

value of $B(CL)\uparrow$ equal to $760\pm80\ e^2\text{fm}^4$. This is in excellent agreement with our result of $744\pm20\ e^2\text{fm}^4$. Inelastic alpha particle scattering measurements[4] have provided values of the isoscalar reduced transition probabilities, $B(OL)\uparrow$, expressed in terms of single particle units for the 1345 (2^+), 2610 (4^+), 3276 (2^+), and 3561 (3^-) keV states. Evaluating these with the Woods-Saxon model (SW[1] in Ref. 4) and the radius $R=1.24\ A^{1/3}$ fm, required for that analysis, allows us to compute values for the isoscalar $B(OL)\uparrow$.

In terms of the results given in Table 7 of Ref. 4 we use

$$B(OL)\uparrow=(2L+1)G_L B(SP)\downarrow=\frac{9R^{2L}}{4\pi}\frac{(2L+1)^2}{(L+3)^2}G_L\ ,$$

where G_L denotes the number of single-particle units.

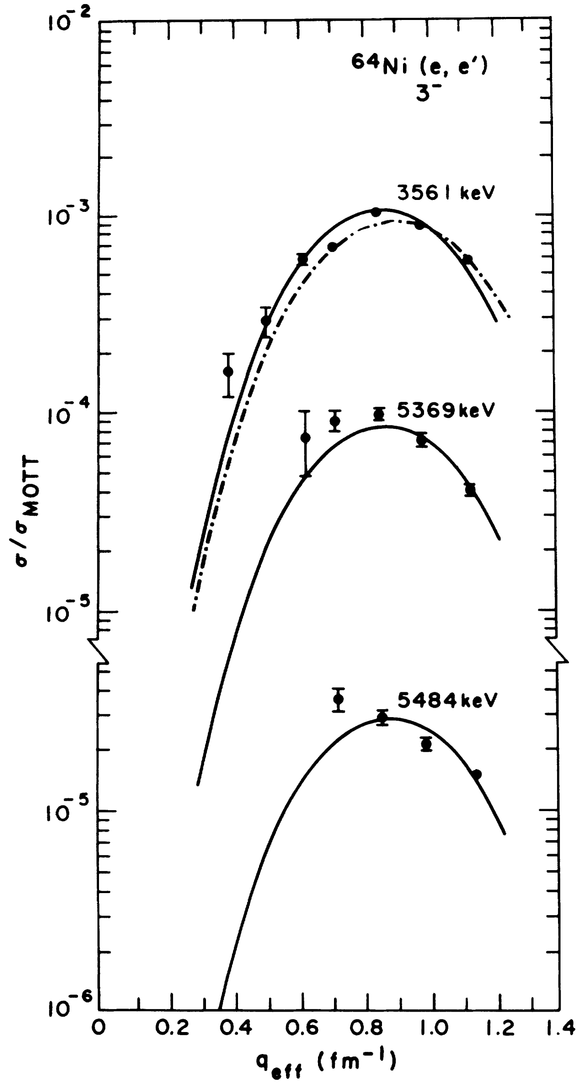

FIG. 5. Comparison of the calculated and measured form factors for the transitions to the states in ^{64}Ni that are thought to have a spin and parity of 3^-. Solid curves are from the Tassie model and the dashed curves assume a phonon transition density.

Electric and isoscalar matrix elements are defined from

$$e^2|M_Z|^2=B(CL)\uparrow\ ,$$

$$|M_0|^2=B(OL)\uparrow\ .$$

In the limit of a hydrodynamic oscillator these will be in the ratio $M_Z/M_0=Z/A$. Inelastic pion scattering results on ^{90}Zr and ^{118}Sn have been expressed in such terms[12] and the collective transitions to the lowest 2^+ and 3^- states of several nuclei have been found to agree with this expectation. For $T=0$ targets electric and isoscalar strengths are also found to agree with this simple expression.[13]

Table II lists the matrix elements M_Z from the present work and M_0 from Ref. 4 for three transitions of ^{64}Ni, all using the single phonon vibrational model for consistency. The ratios for the first 2^+ and 3^- excitations are not in good agreement with the hydrodynamic expectation of $Z/A=0.438$ for ^{64}Ni. While the calculated value of 0.42 for the 2610 keV 4^+ transition is near the hydrodynamic value, the isoscalar analysis for $L=4$ transitions is very sensitive to the radius assumed and the value quoted has a large uncertainty.

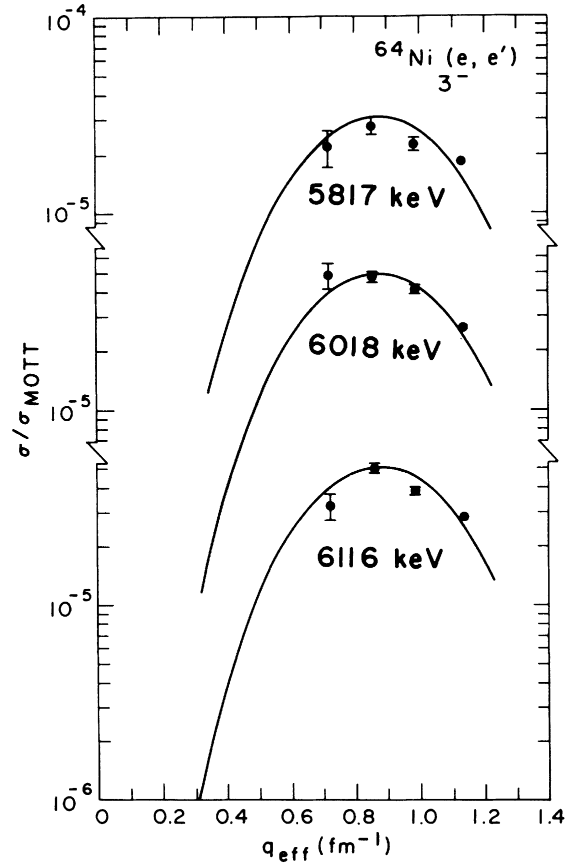

FIG. 6. Comparison of the calculated and measured form factors for the transitions to the states in ^{64}Ni that are thought to have a spin and parity of 3^-. Solid curves are from the Tassie model.

IV. DISCUSSION

The reliable method of inelastic electron scattering with good resolution has been used to determine for the first time the spectroscopic features of a number of states in ^{64}Ni. Data points were insufficient to permit a full determination of the transition densities, but good fits

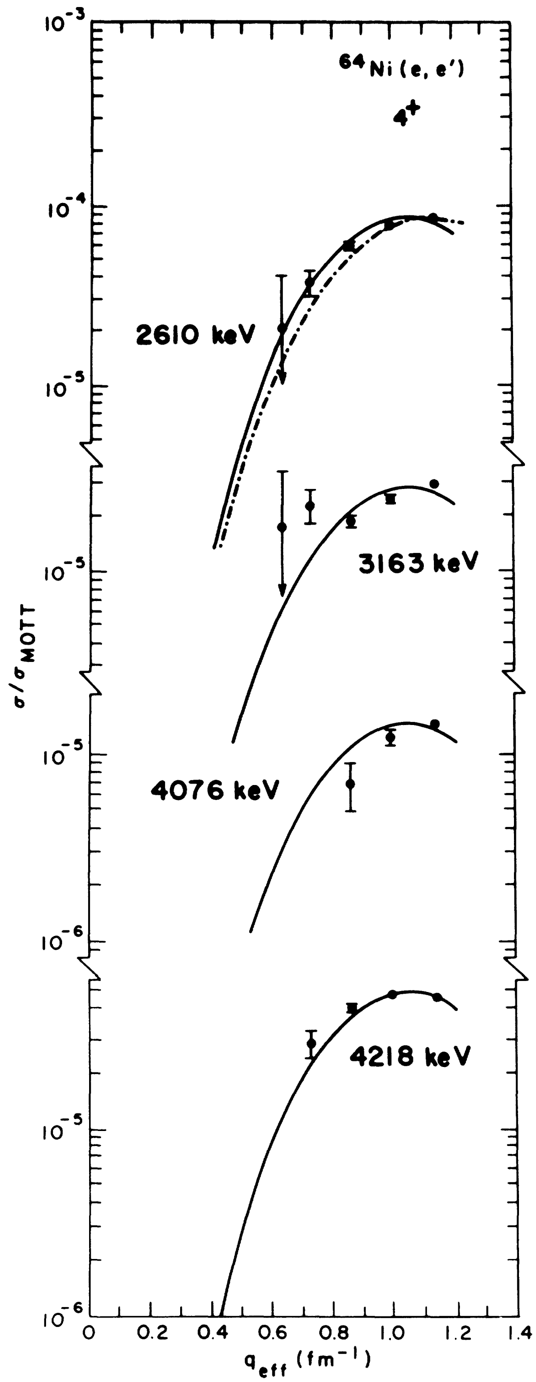

FIG. 7. Comparison of the calculated and measured form factors for the transitions to the states in ^{64}Ni that are though to have a spin and parity of 4^{+}. Solid curves are from the Tassie model and the dashed curves assume a phonon transition density.

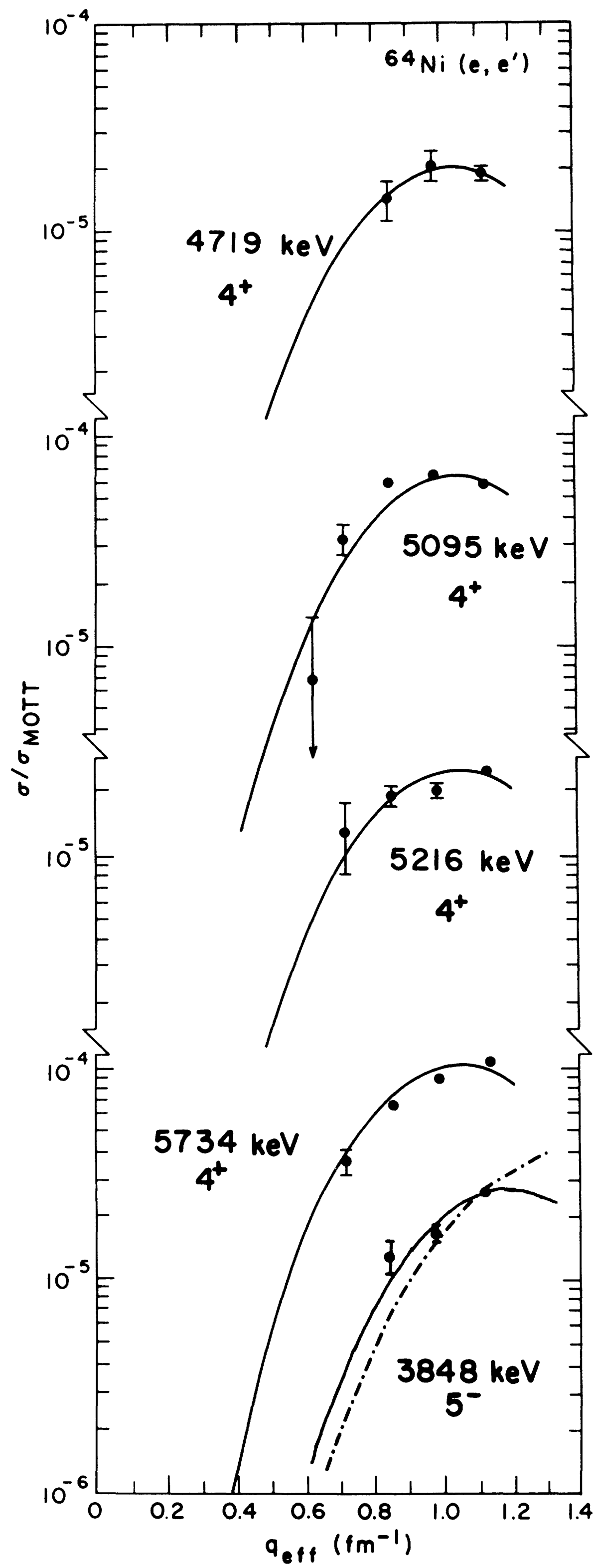

FIG. 8. Comparison of the calculated and measured form factors for the transitions to the states in ^{64}Ni that are though to have a spin and parity of 4^{+} or 5^{-}. Solid curves are from the Tassie model.

TABLE II. Matrix elements, in fm^L, for charge and isoscalar transitions in ^{64}Ni are presented and their ratios are compared to the hydrodynamic model value of $M_Z/M_0 = Z/A = 0.44$. Single-phonon transition densities are used for both the electron and alpha particle scattering. G_L is the isoscalar single-particle enhancement. The errors quoted on M_Z are statistical only. The model dependence is discussed in the text.

State	E_x (keV)	M_Z[a]	G_L[b] (IS)	M_0[b]	M_Z/M_0
2^+	1345	26±0.4	10.3	67± 2	0.39±0.01
4^+	2610	365±5	1.65	860±25	0.42±0.02
3^-	3561	143±2	13.6	450±14	0.32±0.01

[a]Present work.
[b]See Ref. 4.

were obtained in comparing the data to form factors computed with a collective Tassie model. The present $B(C2)\uparrow$ value from the Tassie analysis implies a lifetime of 1.24±0.03 psec, compared to the adopted[11] value of 1.22±0.13 psec.

It would be expected from a collective (hydrodynamic) model for the lowest 2^+ and 3^- states that the reduced charge and isoscalar transition probabilities are related by a simple factor of $(Z/A)^2$. These collective transitions are enhanced by over a factor of 10 above the single-particle estimate, as listed in Table II. Since the collective features of low-lying states are coupled to the giant resonances, it is important to document both the low-lying and giant resonance features of nuclei. The present results provide a portion of the information needed for a consistent study of the collective features of the $Z=28$ nickel isotopes.

Previously available electron scattering and isoscalar alpha particle[4] scattering data are also available for the 2_1^+ and 3_1^- states of ^{58}Ni, ^{60}Ni, and ^{62}Ni. These were compared in just the same fashion as above for ^{64}Ni for a systematic presentation of M_Z, M_0, M_Z/M_0, and the hydrodynamic ratio $(M_Z/M_0)/(Z/A)$. Single phonon, not Tassie transition densities, were used for these comparisons since the isoscalar results use only this model. Uncertainties for the M_0 results are taken from the

TABLE III. Isoscalar and charge matrix elements (in units of fm^{2L}) are compared for the lowest 2^+, 3^-, and 4^+ states of four nickel isotopes, using phonon transition densities. Their ratios M_Z/M_0 are compared to the hydrodynamic expectations of Z/A. Isoscalar results are from Ref. 4. A recent alpha scattering experiment on the nickel isotopes at 25 MeV (Ref. 18) gives slightly smaller values for M_0 for the 2^+ states and appreciably smaller values for the 3^- states. The trends discussed in the text are unchanged if these newer values are used.

	^{58}Ni[a]	^{60}Ni[b]	^{62}Ni[c]	^{64}Ni[d]
2_1^+ E_x (keV)	1454	1333	1173	1345
M_0	63.6±1.2	71.45±4.4	73.8±0.6	67±2
M_Z	24.9±0.6	28.1±0.9	28.2±0.4	26.0±0.4
M_Z/M_0	0.39±0.01	0.39±0.03	0.38±0.01	0.39±0.01
$(M_Z/M_0)/(Z/A)$	0.81±0.02	0.84±0.06	0.85±0.02	0.90±0.03
3_1^- E_x (keV)	4470	4040	3757	3561
M_0	389±3	355±11	455±2	450±14
M_Z	101±2	105±12	117±4	143±2
M_Z/M_0	0.259±0.006	0.29±0.04	0.258±0.009	0.32±0.01
$(M_Z/M_0)/(Z/A)$	0.54±0.01	0.63±0.06	0.57±0.02	0.73±0.03
4_1^- E_x (keV)	2459	2506	2336	2610
M_0	1083±82	1201±120	1593±100	860±25
M_Z	247±14	298±39		365±5
M_Z/M_0	0.23±0.03	0.25±0.05		0.42±0.02
$(M_Z/M_0)/(Z/A)$	0.48±0.06	0.53±0.08		0.95±0.04

[a]Electron scattering results from Ref. 17, corrected for the difference between model-independent and phonon analyses.
[b]Model-independent electron scattering results from Ref. 15, corrected for the difference from a phonon model as found for ^{64}Ni.
[c]Model-independent electron scattering results from Ref. 16, corrected as above.
[d]Present electron scattering results, using a phonon transition density.

difference between the $(SW)^1$ and $(SW)^2$ results of Ref. 4, representing the systematic dependence on the reaction model. Electron scattering results are from Ref. 14 (^{58}Ni), Ref. 15 [^{60}Ni, averaged to give $B(C2)=871$ e^2fm^4], and Ref. 16 (^{62}Ni). All Tassie and model-independent results have been scaled by the factors listed above for the single-phonon model relative to the Tassie model, for each multipolarity. Since different models are used for these different reactions, no clearly consistent analysis can be performed here. These single-phonon charge matrix elements are listed in Table III, where ratios to the isoscalar matrix elements are also listed.

We note from Table III a systematic trend for the 2_1^+ transition to become nearer the hydrodynamic ratio for heavier nickel isotopes. The relatively small values of M_Z/M_0 imply a neutronlike amplitude for the lighter isotopes. For the 3_1^- transitions, a neutronlike ratio is found, constant for all isotopes except ^{58}Ni. Since the added neutrons increasingly block 1 $\hbar\omega$ promotions from the *s*-*d* shell to the *p*-*f* shell, a rising trend in the hydrodynamic ratio is expected. It is difficult to discern any pattern for the 4_1^+ transitions. Inelastic pion scattering would be valuable to confirm these observations, free of the uncertainty entailed by comparing two such different probes as electron and alpha particle scattering.

ACKNOWLEDGMENTS

This work was supported in part by the U.S. Department of Energy and in part by the Foundation for Fundamental Research on Matter (FOM), which is financially supported by the Netherlands Organization for the Advancement of Pure Scientific Research (ZWO). We wish to thank A. J. C. Burghardt, E. Offerman, J. W. de Vries, L. de Vries, and C. de Jager of NIKHEF-K for their assistance in various aspects of acquiring and analyzing the data. We are also indebted to Professor G. Fricke of the University of Mainz for loaning us the ^{64}Ni target.

*Present address: Sektie Kernfysica, Nationaal Instituut voor Kernfysica en Hoge-Energiefysica, P.O. Box 4395, 1009 AJ Amsterdam, The Netherlands.

[1]M. L. Halbert, Nucl. Data Sheets **28**, 179 (1979).

[2]R. G. Tee and A. Aspinall, Nucl. Phys. **A98**, 417 (1967).

[3]P. Beuzit, J. Delaunay, J. P. Fouan, and N. Cindro, Nucl. Phys. **A128**, 594 (1969).

[4]J. Albinski *et al.*, Nucl. Phys. **A445**, 477 (1985).

[5]R. Jahn, U. Wienands, D. Wenzel, and P. von Neumann-Cosel, Phys. Lett. **150B**, 331 (1985).

[6]C. de Vries *et al.*, Nucl. Instrum. Methods **223**, 1 (1984).

[7]W. T. A. Borghols and A. J. C. Burghardt, NIKHEF-K Internal Report 84-A2 (unpublished).

[8]J. Kelly, C. E. Hyde-Wright, and E. Offerman, private communication.

[9]H. de Vries, C. W. de Jager, and C. de Vries, At. Data Nucl. Data Tables **36**, 453 (1987); H. D. Wohlfahrt, Habilationsschrift, University of Mainz, West Germany, 1976 (unpublished).

[10]J. Heisenberg and H. P. Blok (unpublished).

[11]S. Raman *et al.*, At. Data Nucl. Data Tables **36**, 1 (1987).

[12]J. L. Ullmann *et al.*, Phys. Rev. C **35**, 1099 (1987).

[13]G. J. Wagner, P. Grabmayr, and H. R. Schmidt, Phys. Lett. **113B**, 447 (1982).

[14]R. Klein *et al.*, Nuovo Cimento **76A**, 369 (1983).

[15]P. Anderson, L. P. Eckstrom, and J. Lyttkens, Nucl. Data Sheets **48**, 251 (1986).

[16]M. L. Halbert, Nucl. Data Sheets **26**, 5 (1979).

[17]H. Blok, Ph.D. thesis, Free University, Amsterdam, The Netherlands, 1986.

[18]F. Ballester *et al.*, J. Phys. G **13**, 1541 (1987).